1 **Conditional targeting in mice reveals that hepatic homogentisate 1,2-dioxygenase**

2 **activity is essential in reducing circulating homogentisic acid and for effective therapy**

3 **in the genetic disease alkaptonuria.**

4 Juliette H. Hughes[1]*, Ke Liu[1], Antonius Plagge[2], Peter J.M. Wilson[1], Hazel Sutherland[1],

5 Brendan P Norman[1], Andrew T. Hughes[1,3], Craig M Keenan[1], Anna M. Milan[1,3], Takao

6 Sakai[2], Lakshminarayan R. Ranganath[1,3], James A. Gallagher[1,+·], George Bou-Gharios[1,+].

7

8 [1] Institute of Ageing and Chronic disease, University of Liverpool, Liverpool, L7 8TX, UK; [2]

9 Institute of Translational Medicine, University of Liverpool, Liverpool, L69 3GA, UK; [3]

10 Liverpool Clinical Laboratories, Department of Clinical Biochemistry and Metabolic

11 Medicine, Royal Liverpool and Broadgreen University Hospitals Trust, Liverpool, L7 8XP,

12 UK.

13 [+] JAG and GBG contributed equally.

14

15 Correspondence: *Juliette H Hughes, hljhugh4@liverpool.ac.uk; Address: William Henry

16 Duncan Building, 6 West Derby Street, Liverpool, L7 8TX.

17

18

19

20

21

22

23

24

25

1

26 **Abstract**

27 Alkaptonuria is an inherited disease caused by homogentisate 1,2-dioxygenase (HGD)

28 deficiency. Circulating homogentisic acid (HGA) is elevated and deposits in connective

29 tissues as ochronotic pigment. In this study, we aimed to define developmental and adult

30 HGD tissue expression and determine the location and amount of gene activity required to

31 lower circulating HGA and rescue the alkaptonuria phenotype.

32

33 We generated an alkaptonuria mouse model using a knockout-first design for the disruption

34 of the HGD gene. Hgd tm1a -/- mice showed elevated HGA and ochronosis in adulthood.

35 LacZ staining driven by the endogenous HGD promoter was localised to only liver

36 parenchymal cells and kidney proximal tubules in adulthood, commencing at E12.5 and

37 E15.5 respectively. Following removal of the gene trap cassette to obtain a normal mouse

38 with a floxed 6th HGD exon, a double transgenic was then created with Mx1-Cre which

39 conditionally deleted HGD in liver in a dose dependent manner. 20% of HGD mRNA

40 remaining in liver did not rescue the disease, suggesting that we need more than 20% of liver

41 HGD to correct the disease in gene therapy.

42

43 Kidney HGD activity which remained intact reduced urinary HGA, most likely by increased

44 absorption, but did not reduce plasma HGA nor did it prevent ochronosis. In addition,

45 downstream metabolites of exogenous $^{13}C_6$-HGA, were detected in heterozygous plasma,

46 revealing that hepatocytes take up and metabolise HGA.

47

48 This novel alkaptonuria mouse model demonstrated the importance of targeting liver for

49 therapeutic intervention, supported by our observation that hepatocytes take up and

50 metabolise HGA.

51 **<u>Introduction</u>**

52 Alkaptonuria (AKU; OMIM #203500) is a rare metabolic recessive disease where the

53 enzyme homogentisate 1,2-dioxygenase (HGD; EC 1.13.11.5), that is mainly found in the

54 liver, is deficient (1). Garrod in 1908 unveiled the term *inborn error of metabolism* and

55 proposed that AKU was caused by the lack of an enzyme that in normal individuals split the

56 aromatic ring of homogentisic acid (HGA) (2). Biochemical evidence of the defect in AKU

57 was provided by La Du in 1958, where he demonstrated the absence of HGD activity in a

58 liver homogenate prepared from an AKU patient and established that the failure to synthesize

59 active enzyme was the sole cause of AKU (1).

60

61 HGD deficiency leads to HGA accumulation in the blood and tissues, despite urinary

62 excretion. It has been proposed that excess HGA undergoes oxidation and polymerization to

63 form a dark brown ochronotic pigment (3) that deposits in connective tissues such as the skin,

64 sclera, spine and articular cartilage, as well as in heart valves (4, 5), where it causes aortic

65 stenosis (6). AKU patients suffer from early-onset severe osteoarthropathy due to premature

66 degeneration of articular cartilage and disease manifestations worsen with age. Despite liver

67 deficiency of HGD, the main pathophysiological manifestation of AKU relates to the

68 function of non-metabolised HGA in the joints.

69

70 HGD has been mapped onto human chromosome 3q13.33

71 (http://www.ncbi.nlm.nih.gov/gene/3081) (7, 8). Currently, 203 different HGD pathogenic

72 variants have been identified (HGD mutation database: http://hgddatabase.cvtisr.sk) (9, 10),

73 of which the most frequent are missense variants (representing 68.3%), followed by splicing

74 (13.4%) and frameshift (11.3%) mutations (11). In addition to the liver, HGD is thought to be

75 expressed in the prostate, small intestine, colon, and kidney (12), as well as in osteoarticular

76   compartment cells (chondrocytes, synoviocytes, and osteoblasts) (13), and the brain (14).

77   However, this has not been verified by in-situ hybridisation or HGD labelling.

78

79   Currently, AKU treatment is palliative via analgesics and joint replacement, with dietary

80   protein restriction and vitamin C showing little or no efficacy (15). Recently there have been

81   trials of 2-(2-nitro-4-trifluoromethylbenzoyl)-1,3-cyclohexanedione (NTBC), more

82   commonly referred to as nitisinone, in the treatment of AKU (16). Nitisinone, which inhibits

83   the HGA producing enzyme 4-hydroxyphenylpyruvate dioxygenase (HPPD; EC 1.13.11.27),

84   has been the licensed treatment for hereditary tyrosinaemia type 1 (HT-1; OMIM #276700)

85   since 2002, where fumarylacetoacetate hydroxylase (FAH; EC 3.7.1.2) deficiency results in

86   liver failure, hepatocellular carcinoma and renal tubular dysfunction (17). Moreover, the off-

87   licence use of nitisinone at the National Alkaptonuria Centre (Liverpool, UK) has shown a

88   decreased rate of disease progression in addition to lowering serum and urine HGA (18).

89

90   Treatment of other inborn errors of metabolism related to the phenylalanine/tyrosine pathway

91   by enzyme replacement has been attempted with some success (19). In the past decade, liver-

92   directed gene therapy has emerged as a promising alternative to transplantation in monogenic

93   liver disorders such as AKU (20). The level of HGD required to rescue the disease, if

94   expression outside the liver can affect the phenotype and whether circulating HGA can be

95   metabolised by HGD-expressing cells are essential questions that must be addressed before

96   such treatments are investigated.

97

98   To answer these questions, a new targeted knockout-first AKU mouse model was generated.

99   This mouse harbours a LacZ reporter gene within the HGD locus for localising gene

100   expression and was conditionally manipulated to obtain an inducible and liver-specific

101   knockout. This study provides compelling evidence that targeting hepatic HGD plays an

102   indispensable role in any enzyme replacement or gene therapy for AKU.

103

104   **Results**

105   <u>Generation of the conditionally targeted Hgd mouse</u>

106   ES cells from clone C10 resulted in chimeras which achieved germline transmission. This

107   knockout-first allele (Hgd tm1a) contained an IRES:LacZ gene trap cassette and a promoter-

108   driven neo cassette inserted into the fifth HGD intron with the sixth exon flanked by loxP

109   sequences, see figure 1A (21, 22). Homozygous Hgd tm1a mice showed an AKU phenotype

110   due to HGD gene disruption. In C10/tm1a mice, Lox-F/Hgd-R primers amplified the loxP

111   sequence (257bp) showing the allele was floxed (figure 1). Hgd-F/Hgd-ttR primers produced

112   a 561bp band in the wildtype allele; the gene trap cassette sequence in the modified allele was

113   too large to be amplified. Homozygous tm1a therefore had only the 257bp floxed band,

114   heterozygotes had both the floxed 257bp and wildtype 561bp bands and wildtype had only

115   the 561bp band (figure 1B).

116

117   Hgd tm1c had restored HGD gene expression due to removal of the gene trap and was

118   phenotypically wildtype. To achieve inducible and conditional HGD deletion, interferon

119   inducible Mx-1 was used to drive expression of cre recombinase, MxCre (23), generating the

120   Hgd tm1d allele. In the post-flp tm1c and tm1d (before cre recombination), Lox-F/Hgd-R

121   primers showed the allele was floxed (257bp) and Hgd-F/Hgd-ttR primers showed that Flp

122   recombination had occurred (673bp). Wildtype tm1c/d had only the 561bp band (Hgd-F/Hgd-

123   ttR). Homozygous tm1c/d had both the 257bp floxed and 673bp post-flp bands and

124   heterozygous tm1c/d had all three bands (257bp floxed, 673bp post-flp and 561bp wildtype),

125   see figure 1C. Primers produced a band at 520bp when MxCre was present (figure 1D).

126

127 <u>Elevation of HGA in plasma and urine</u>

128 HGA was measured in urine and plasma of mice (figure 1E-F). Urinary HGA (mean ±SEM)

129 was elevated approximately 100,000-fold (99,575 ±30,851µmol/L) and plasma HGA

130 elevated about 100-fold (100.5 ±34.9µmol/L) in the Hgd tm1a -/- mice compared to Hgd

131 tm1a -/+ (plasma: 2.0 ±0.5µmol/L; urine: 15 ±25.3µmol/L), Hgd tm1c (plasma: 2.0

132 ±1.0µmol/L; urine: 2.4 ±2.9µmol/L) and C57BL/6 wildtype (plasma: 1.7 ±0.6µmol/L; urine:

133 0.8 ±0.2µmol/L) mice. These differences were all statistically significant (p<0.001; one-way

134 ANOVA, Tukey-Kramer post-hoc).

135

136 As AKU is present at birth, plasma HGA was measured in day 1 Hgd tm1a -/- pups (2 pools

137 of n=3; gestation: 19.5 days), see figure 1G. Plasma HGA (mean ±SEM) was elevated 3-fold

138 in day 1 pups (308.8 ±18.9µmol/L) compared with adult Hgd tm1a -/- mice (100.5

139 ±8.7µmol/L).

140

141 <u>Detection of ochronosis and its progression</u>

142 Knee joints from Hgd tm1a -/- mice aged 7–40 weeks were examined for pigmentation.

143 Ochronosis was found in calcified articular cartilage (figure 2A), first appearing at 9 weeks

144 (figure 2B). The pigment was initially pericellular (9-11 weeks) and very infrequent. At 26

145 and 40 weeks (figure 2C and 2E respectively), the number and intensity of pigmented

146 chondrons were increased and showed advancement to the intracellular compartment.

147 Clusters of pigmented chondrons were seen at ligament attachment sites (not shown). At 40

148 weeks, pigmentation was still confined to calcified cartilage. Heterozygous controls showed

149 no pigmentation at 26 and 40 weeks (figure 2D and 2F respectively).

150

151   Adult HGD expression

152   Adult tissues from Hgd tm1a -/- were stained for LacZ to visualise HGD expression as blue

153   staining. Positive staining was present in the liver and kidney cortex after 2 hours which

154   intensified when left overnight (figure 3A). Heterozygous staining was less intense (not

155   shown) and was slower to develop. Hgd tm1c wildtype-like liver and kidney did not stain

156   (figure 3A). All other Hgd tm1a tissues investigated including brain, heart, lung, muscle,

157   spleen, intestine, skin, bone, cartilage, eye and prostate were negative. HGD mRNA analysis

158   via qPCR (HGD1 primers spanning exons 3-4 before gene trap cassette) confirmed this

159   staining pattern, with HGD expression only present in liver and kidney (figure 3B).

160

161   LacZ in whole liver and kidney was limited by the penetration of substrate therefore frozen

162   section staining was undertaken to demonstrate that LacZ and therefore HGD is expressed in

163   the cytoplasm throughout the liver parenchyma (figure 3C). In the kidney cortex, glomeruli

164   were LacZ negative, and only certain tubules stained positive (figure 3D), which were

165   identified using periodic acid schiff for brush border staining in proximal convoluted tubules

166   (PCT) (figure 3E,F).

167

168   Embryonic HGD expression

169   To determine when HGD is expressed, LacZ staining of time-mated Hgd tm1a -/- embryos

170   was carried out. Whole embryo staining showed positive LacZ staining in the liver at E14.5

171   and onwards (figure 3G). However, histological sections revealed punctate staining at E12.5

172   and onwards in the liver (figure 3H). Positive LacZ staining was seen in the kidney at E15.5

173   in some of the developing kidney tubules (figure 3H). All other embryonic tissues examined

174   in frozen sections, including brain, eye, bones and other internal organs were LacZ negative.

175

176   Similarly, liver HGD mRNA expression in Hgd tm1a -/- (HGD1 primers spanning exons 3–4

177   before gene trap cassette) was analysed by qPCR (figure 3I) at E12.5 (n=3), E13.5 (n=3),

178   E14.5 (n=4) and E15.5 (n=3), day 1 pups (n=6) and compared with adult mice (n=4, male,

179   mean age 19.7 weeks). Compared to the adult, liver HGD expression was 0.3% at E12.5,

180   0.8% at both E13.5 and E14.5, and 2.3% at E15.5. This considerable difference in HGD

181   mRNA was reflected in the LacZ staining intensity seen between the adult liver (figure 3C)

182   compared to the embryo liver (figure 3H). Day 1 pup liver HGD expression was 12.6% of the

183   adult expression level (8-fold lower).

184

185   <u>Inducible and liver-specific HGD knockout</u>

186   To investigate the effect of liver-specific HGD gene deletion, double transgenic Hgd tm1d

187   MxCre +ve mice (n=5) and wildtype (n=3) and AKU (n=4) controls were injected with pIpC.

188   Blood and urine samples were collected according to the scheme in figure 4A. 15 days after

189   the first pIpC injection, MxCre +ve mice showed a 77.6% decrease in liver HGD mRNA

190   compared with wildtype controls (figure 4B). Kidney HGD expression in MxCre +ve mice

191   did not change and was comparable to wildtype controls (figure 4C). AKU mice had no HGD

192   mRNA expression as expected (primers span exons 9–10 after gene trap cassette).

193

194   Following the knockout of approximately 78% liver HGD mRNA in MxCre +ve mice, mean

195   plasma HGA (±SEM) increased from 0.2 ±0.2µmol/L to 129.3 ±35.6µmol/L at 15 days post-

196   pIpC (figure 4D). MxCre +ve urinary HGA (figure 4E) was elevated from 9.4 ±7.1µmol/L to

197   11,807 ±974µmol/L at 15 days post-pIpC but remained low in comparison to AKU controls

198   (134,948 ±18,479µmol/L). Both plasma and urinary HGA remained high in AKU controls

199   and low in wildtype controls as expected.

200

201   Long-term liver-specific HGD knockout

202   MxCre +ve mice (n=15) and AKU controls (n=5) were injected with pIpC. MxCre +ve

203   wildtype controls were injected with PBS (n=5) as wildtype controls. Injections and sampling

204   of blood and urine was carried out according to the scheme in figure 5A. MxCre +ve mice

205   injected with pIpC were culled at 9 (n=5), 15 (n=5) and 20 (n=5) weeks post-injection, with

206   wildtype and AKU controls culled at 20 weeks. Liver and kidney mRNA was taken and knee

207   joints were taken to assess ochronosis.

208

209   As with the previous study, liver HGD mRNA was reduced in pIpC-injected MxCre +ve

210   mice, which was sustained to 20 weeks post-injection, see figure 5B. Compared to wildtype

211   controls, liver HGD expression was 11.7%, 17.7% and 18.4% at 9, 15 and 20 weeks

212   respectively. Kidney HGD expression in the MxCre +ve mice remained comparable to

213   wildtype controls (figure 5C). The reduction of liver HGD mRNA in the MxCre +ve mice

214   subsequently caused plasma HGA to increase (figure 5D) to a level comparable with AKU

215   controls. Urinary HGA (figure 5E) was increased in the MxCre +ve mice but not to that of

216   AKU controls. Knee sections stained with Schmorls' stain were scored to obtain the number

217   of pigmented chondrons found in a representative knee joint section (figure 5F). Few or no

218   pigmented chondrons were found in the MxCre +ve knee joints 9 weeks post-pIpC,

219   increasing in number at 15 and 20 weeks. Wildtype controls showed no pigmentation.

220

221   Liver-specific HGD knockout: dose response

222   In order to investigate the effect of varying liver HGD mRNA expression levels on the AKU

223   phenotype, a short term dose response study was carried out. Figure 6A demonstrates the

224   study design. MxCre +ve mice were given two injections of pIpC at the following doses;

225   3.33μg/g (n=3), 1μg/g (n=3), 0.33μg/g (n=3), 0.1μg/g (n=5), 0.03μg/g (n=3) and 0.01μg/g

226 (n=3) body weight. AKU (Hgd tm1a -/-; n=4) and wildtype (MxCre WT; n=7) controls were

227 given the highest dose of 3.33µg/g pIpC. With the exception of the 0.01µg/g group, liver

228 HGD mRNA in MxCre +ve mice was reduced at 15 days post-injection (figure 6B) in all

229 groups, with a dose response observed at the lower pIpC doses. The mean liver HGD

230 expression in MxCre +ve mice 15 days post-pIpC compared to wildtype controls was

231 lowered to 17.0%, 20.5%, 20.5%, 53.4% and 54.5% with decreasing pIpC doses from

232 3.33µg/g – 0.03µg/g. The mean liver HGD expression in the 0.01µg/g group was comparable

233 to the WT controls. Kidney HGD expression was unchanged (figure 6C).

234

235 Plasma HGA in MxCre +ve mice at 15 days post-pIpC were lowered in a dose responsive

236 manner (mean ±SEM) to 75.0 ±20.9, 57.9 ±20.9, 27.2 ±9.6, 22.7 ±13.4, 26.1 ±24.1 and 1.3

237 ±0.4 µmol/L with decreasing pIpC doses (figure 6D). Similarly, urine HGA demonstrated a

238 dose response at 15 days post-pIpC, at (mean ±SEM) 45,074 ±14,977, 14,169 ±13,783, 6,137

239 ±6,064, 5,717 ±5,667, 31,043 ±31,041 and 2.0 ±0.2 µmol/L with decreasing pIpC doses

240 (figure 6E). These levels of urine HGA were elevated compared with wildtype (1.9 ±0.2

241 µmol/L) controls, but lower than AKU (113,067 ±10,609 µmol/L) controls. Figure 6F-G

242 show the relationship between liver HGD mRNA (expressed as percentage of the mean

243 wildtype level) and HGA.

244

245 <u>Metabolism of circulating HGA</u>

246 To determine if circulating HGA can be taken up by HGD-expressing cells to be metabolised

247 intracellularly, both Hgd tm1a -/- (n=4) and Hgd tm1a -/+ (n=4) mice were injected with

248 $^{13}C_6$-HGA into the tail vein. Plasma samples were then collected at various time points, from

249 2–60 minutes post-injection. HGA in its native form (m+0) was detected in plasma of Hgd

250 tm1a -/- mice at all time points, and was absent in Hgd tm1a -/+ mice (not shown). $^{13}C_6$-HGA

251   was detected in both Hgd tm1a -/- and -/+ mice after injection (figure 7). M+6 isotopologues

252   of fumarylacetoacetic acid ($^{13}C_6$-FAA)/maleylacetoacetic acid ($^{13}C_6$-MAA), $^{13}C_6$-labelled

253   downstream metabolites, were detected in Hgd tm1a -/+ mice after $^{13}C_6$-HGA injection, and

254   were not detected in Hgd tm1a -/- mice. Native FAA/MAA was not detected in either Hgd

255   tm1a -/- or -/+ mice (not shown).

256

257   **<u>Discussion</u>**

258   Management of inborn errors of metabolism such as AKU has traditionally consisted of diet

259   and supportive therapy. However, other treatment options have become available, including

260   enzyme inhibition (17, 24), enzyme replacement (19), cell and organ transplantation (20),

261   gene therapy (20) and CRISPR technology (25).

262

263   The pathophysiology of AKU has been investigated in *ex vivo* tissue samples (14, 26, 27) and

264   *in vitro* models (13, 28) but to investigate the metabolic consequences of AKU and novel

265   therapeutic approaches, we have generated a well-characterised animal model. This model

266   will be used to investigate all aspects of AKU pathophysiology including the mechanism of

267   ochronosis and any associated tissue changes including amyloidosis (29). We have generated

268   a HGD knockout-first mouse model that included a beta galactosidase (LacZ) gene trap

269   within the HGD gene locus, that has enabled precise localistation of HGD expression.

270   Targeted gene disruption in Hgd tm1a removes any potentially confounding mutations that

271   could be present in an existing ENU (N-ethyl-N-nitrosourea) AKU mouse model (30), as

272   ENU mutagenesis causes a high frequency of genomic mutations (31). This new mouse

273   recapitulated the human disease. Manipulation of this Hgd tm1a knockout-first allele by

274   FRT/flp and Cre/loxP recombination enabled liver-specifc HGD deletion in double transgenic

275 Hgd tm1d MxCre +ve mice, highlighting important considerations for future therapy in

276 AKU.

277

278 Plasma HGA in Hgd tm1a -/- is comparable to that previously reported values in the ENU

279 AKU mouse (30). This mutagenesis model exhibited the first signs of ochronosis at 15 weeks

280 (30). Knee joints were therefore examined from 7-11 weeks in Hgd tm1a -/- mice, with

281 pericellular pigmentation identified at 9 weeks; progression was then similar to mutagenesis

282 AKU mice. Ochronosis in the mouse appears to represent the early stages of human joint

283 pathophysiology in AKU with pigmentation confined to individual chondrocytes and their

284 territorial matrix in the calcified cartilage.

285

286 The LacZ reporter gene has enabled both temporal and spatial histological localisation of

287 HGD showing that HGD was expressed throughout the liver parenchyma and kidney PCT

288 cells. It has previously been suggested that HGD is expressed in the intestine and prostate

289 (12), brain (14) and bone/cartilage (13), but this was not evident using this knock-in LacZ

290 reporter gene, nor by qPCR analysis of HGD mRNA.

291

292 LacZ staining of time-mated embryos demonstrated that hepatic HGD expression begins at

293 E12.5 (figure 3H), confirmed with qPCR analysis of liver HGD mRNA from E12.5-E15.5.

294 Hepatic cords, containing hepatoblasts, have formed by E10.0 in the developing liver

295 alongside haematopoietic cells. The liver then expands due to hepatoblast proliferation and

296 haematopoietic activity from E10.5-E11.5 (32). Haematopoietic activity rapidly increases,

297 peaking at E13.5 and does not start to decline until E15.5 (32). Haematopoietic cells

298 encompass almost 75% of total liver volume at E13.0 (33) with hepatoblasts at E13.5 having

299 limited contact with each other (32), explaining the diffuse and punctate LacZ staining and

300 low HGD mRNA level in the embryonic liver. Murine hepatoblasts begin to differentiate into

301 hepatocytes at E14.5 (32). Haemaotpoietic activity continues into the first post-natal week,

302 which may explain why day 1 pups have about an eighth of adult HGD expression (32). In

303 the kidney, adult LacZ staining suggests that the LacZ positive cells seen at E15.5 are

304 developing PCT cells of the nephron.

305

306 HGD expression begins in embryonic development. The 3-fold greater HGA level seen at

307 birth compared to adulthood in Hgd tm1a -/- mice (figure 1G) highlights the importance of

308 HGD, even at this very early time point, perhaps suggesting that therapeutics strategies, such

309 as nitisinone (16) or gene/enzyme replacement should ideally begin in early life or at birth.

310

311 <u>Liver-specific HGD deletion</u>

312 To investigate contribution of non-hepatic HGD towards HGA metabolism, double

313 transgenic mice were generated by mating floxed Hgd tm1d mice with an MxCre

314 recombinase line, and used for liver-specific HGD deletion (23, 34). Two doses of 10μg/g

315 body weight pIpC (figure 4,5) resulted in an approximate 80% reduction in liver HGD

316 mRNA, whilst kidney HGD mRNA was maintained at the wildtype level. This reduction of

317 liver HGD mRNA and subsequent increase in plasma HGA to a level comparable with AKU

318 controls suggests that hepatic HGD is crucial for HGA metabolism.

319

320 These results indicate that future gene/enzyme replacement therapy should target the liver to

321 combat elevated plasma HGA that causes ochronosis in AKU. This is supported by a case

322 report of an AKU patient receiving a liver transplant, after which they found no HGA in the

323 urine and reported a halt in progressive arthropathy (35). Full liver HGD mRNA knockout

324 was not achieved with two 10μg/g doses in the present study. Further reducing liver HGD

325   mRNA, would not provide further insight into the level of liver HGD mRNA required to

326   rescue the phenotype.

327

328   The data here reveals that approximately 20% liver HGD mRNA, delivered by gene therapy

329   for example, will not rescue AKU; elevated HGA subsequently caused ochronosis in the knee

330   joints of the mice (figure 5F). Determining how much liver HGD is required to rescue the

331   phenotype is an important question for future therapy. The dose response study here (figure

332   6) intended to estimate how much liver HGD mRNA would significantly lower circulating

333   HGA. A dose response was observed in both the plasma and urine HGA levels (figure 6D,E).

334   However, for liver HGD mRNA, there was only a dose response between 0.33-0.01µg/g

335   pIpC. One possible explanation for HGD mRNA not corresponding to plasma HGA in the

336   other dose groups could be that the mRNA:protein ratio is not linear. Thus we suggest that

337   the minimum level of liver HGD mRNA required to eliminate circulating HGA must fall

338   between the dashed lines (figure 6F), between 26% and 43% of liver HGD mRNA.

339

340   The intact kidney HGD mRNA did not have an impact on plasma HGA, but instead caused

341   reduced urinary HGA compared to AKU controls. In 2002, an AKU patient who received a

342   kidney transplant reportedly had normalised plasma HGA and decreased urinary HGA (both

343   approximately half pre-transplant levels) (36). Liver-specific HGD deletion shown here in

344   mice however suggests that kidney HGD mRNA is unlikely to rescue the AKU phenotype as

345   blood HGA levels were elevated. The improvement reported with kidney transplantation was

346   likely due to improved renal elimination as the patient had renal failure and subsequently

347   very high HGA pre-transplant, rather than donor HGD expression. Indeed, in the conditional

348   mouse model (figures 4-5) we were expecting high HGA in the urine when circulating HGA

349   increased. However, in the liver-specific knockout, the urine level did not increase,

350   suggesting HGA reabsorption and subsequent metabolism by the intact kidney HGD, for

351   which we do not know the mechanism. Fundamentally, the importance of this finding is that

352   intact kidney HGD does not rescue the disease and therefore liver HGD is critical for the

353   correction of AKU.

354

355   <u>HGD activity and HGA metabolism: considerations for gene therapy</u>

356   Restoring HGD activity in all liver cells, via gene therapy or enzyme replacement, is

357   unachievable by any current method, but the data here suggests that it is not necessary. In

358   heterozygous mice and humans, one functioning copy of the HGD gene in all cells is

359   sufficient to deal with HGA metabolism. Assuming heterozygous mice possess 50% of the

360   HGD mRNA compared with wildtypes (adult LacZ staining suggests this assumption is

361   correct), then 50% HGD mRNA in every hepatocyte can rescue AKU. As described above,

362   conditional deletion to 20% of total HGD liver mRNA, did not appear to rescue the

363   phenotype. However, we cannot determine how many cells were expressing the gene, either

364   as one or two alleles, nor the distribution of expression which could be variable from cell to

365   cell. The proportion of corrected cells and the level of therapeutic gene expression per cell

366   required to rescue AKU is therefore still not clear. A recent study providing the first human

367   genotype-phenotype correlation data for the three most frequent HGD mutation variants (33

368   patients homozygous for these variants) identified in the SONIA-2 trial demonstrated no

369   difference in baseline visit serum or 24-hour urine HGA, or clinical symptoms such as eye

370   pigmentation, hip bone density or degree of scoliosis between patients predicted to have 1%

371   (16 patients) or 31%-34% (17 patients) residual HGD catalytic activity as determined *in vitro*

372   against wildtype recombinant human HGD enzyme) (9).

373

374   Another consideration for gene therapy is that hepatocytes without sufficient HGD activity to

375   metabolise HGA could lead to its accumulation in the bloodstream. In this study, intravenous

376   injection of isotopically labelled HGA (figure 7) provides evidence that circulating HGA can

377   re-enter HGD-expressing cells to be metabolised by intracellular HGD. Thus, it should not be

378   necessary to repair 100% of liver cells because HGA produced by AKU hepatocytes could be

379   taken up and metabolised by genetically repaired cells. This model represents a paradigm for

380   inherited liver metabolic diseases, in particular, genetic disorders of tyrosine metabolism.

381

382   Conclusion

383   In summary, this new targeted HGD knockout mouse exhibits the characteristic traits of

384   AKU. Both adult and embryo HGD expression has been localised to only liver and kidney

385   using a reporter gene within the HGD locus. More importantly, the conditional Hgd tm1d

386   MxCre model has highlighted the importance of liver HGD expression in limiting the

387   pathological effects of the HGA pool despite apparent reabsorption of HGA in the kidney.

388

389   **Materials and Methods**

390   Generation of HGD knockout-first mice

391   Two ES cell lines (clones Hgd C10, Hgd C11) were obtained from the UC Davis KOMP

392   repository. They were grown on feeder cells as described (37). Healthy ES colonies were

393   injected into blastocysts of C57BL/6 (Harlan, UK) and chimeras born from both lines. Only

394   C10 chimeras achieved germline transmission. All mice were housed and maintained within

395   the University of Liverpool Biological Services Unit in specific pathogen-free conditions in

396   accordance with UK Home Office guidelines. Food and water were available *ad libitum*.

397

398   Urine and Blood Collection

16

399 Tyrosine pathway metabolites in acidified urine and plasma from venous tail bleeds were

400 analysed via high performance liquid chromatography (HPLC) tandem mass spectrometry

401 assays (38, 39).

402

403 <u>LacZ staining; tissues/embryos</u>

404 Embryos from E13.5 to E16.5 were stained for ß-galactosidase as previously described (40).

405 Adult tissues were stained via the same protocol with size-adjusted fixation times.

406

407 <u>LacZ staining; frozen sections</u>

408 Frozen liver and kidney sections (6μM) were fixed (0.2% glutaraldehyde in PBS) for 10

409 minutes. After three washes in cold PBS they were stained for ß-galactosidase as above and

410 counterstained with eosin. Whole embryos were fixed as above, transferred to 30% sucrose

411 overnight and then embedded in OCT on dry ice. Frozen sections (7μM) were LacZ stained

412 at room temperature overnight.

413

414 <u>qPCR</u>

415 RNA was extracted using the Qiagen RNeasy Mini Kit, reverse transcription of RNA was

416 carried out using the Applied Biosystems RNA-to-cDNA kit and qPCR was performed using

417 the Bio-Rad iQ™ SYBR® Green Supermix. HGD1 primers; forward 5'-

418 TGTCCACGGAACACCAATAA-3' and reverse 5'- GCCAACTTCATCCCAGTTGT-3'.

419 HGD2 primers; forward 5'-GACCCATCGGAGCAAATGGC-3' and reverse 5'-

420 AGTGTAACCACCTGGCACTC-3'. 18S (housekeeping gene) primer sequences; forward

421 5'-TGTCCACGGAACACCAATAA-3' and reverse 5'-AGTTCTCCAGCCCTCTTGGT-3'.

422 18S was not affected by pIpC administration.

423

424 Ochronosis

425 Coronal knee joint paraffin sections were Schmorl's stained and counterstained with nuclear

426 fast red (28, 41) to identify pigmented chondrons. Scoring of all four joint quadrants was

427 carried out blind to experimental conditions and genotype.

428

429 Hgd tm1d conditional knockout

430 To obtain the conditional Hgd tm1d line, Hgd tm1a mice were crossed with Flpo mice to

431 remove the FRT-flanked gene trap cassette, leaving a floxed target exon (Hgd tm1c) (42).

432 Homozygote floxed Hgd tm1c mice were crossed with MxCre mice. The removal of the

433 floxed 6th exon was induced with two intraperitoneal injections of polyinosinic:polycytidylic

434 acid (pIpC) at 10µg/g body weight (43). Hgd tm1a -/- mice were injected with pIpC as AKU

435 controls and wildtype controls were either Hgd tm1d MxCre WT injected with pIpC or Hgd

436 tm1d MxCre +ve mice with PBS. HGA was measured in plasma and urine samples collected

437 pre-injection and at time points post-injection. Liver and kidney HGD mRNA was analysed.

438 In the long-term study, knee joints were collected for ochronosis scoring. For the dose

439 response study, the same protocol was followed as above, using diluted pIpC at doses

440 3.33µg/g to 0.01µg/g body weight.

441

442 Isotopic HGA injection

443 Hgd tm1a -/- (n=4) and Hgd tm1a -/+ (n=4) mice were injected with $^{13}C_6$-HGA into the

444 lateral tail vein, adjusted to body weight to achieve a final blood concentration of

445 approximately 1mmol/L. Under anaesthesia, venous tail bleeds were collected at time points

446 post-injection, ranging from 2-60 minutes. Whole blood was centrifuged and the supernatant

447 removed and immediately frozen.

448   Non-targeted metabolic flux analysis was performed to trace metabolism of $^{13}C_6$-HGA.

449   Metabolic profiling was performed using a published mass spectrometric technique (44).

450   Briefly, plasma was diluted 1:9 plasma:deionised water and HPLC performed on an Atlantis

451   dC$_{18}$ column (3x100mm, 3μm, Waters, UK) coupled to an Agilent (Cheadle, UK) 6550

452   quadrupole time-of-flight mass spectrometer. An accurate-mass compound database with

453   potential association to HGA was generated for data mining using Agilent Pathways to

454   PCDL. Data were mined for these compound targets with an accurate mass window of

455   ±5ppm using 'batch isotopologue extraction' in Profinder (build 08:00, Agilent).

456   Isotopologue extraction investigates association with the injected $^{13}C_6$-HGA by examining

457   the relative abundances of the M+0 – M+6 isotopologues for compound targets.

458

459   <u>Statistical analysis</u>

460   Statistical analysis was performed using Stats Direct 3 statistical software (UK). Significance

461   is denoted as $p<0.05$ *, $p<0.01$ ** and $p<0.001$ ***.

462

466

467   **Author contributions:** GBG, LRR and JAG designed the study. GBG, KL, AP and JHH

468   established the mouse model. JHH, KL, PJMW, HS, BPN and CMK carried out the

469   laboratory analyses. AT and AM assisted in data acquisition. TS supplied Cre mice and

470   knowledge of pIpC. LRR, JAG and GBG supervised the project. JHH wrote the first draft of

471   the paper. All authors reviewed the content and agreed the final version.

472

473   **Conflict of Interest:** The authors declare no competing interests.

474

475   <u>**References**</u>

476   1. La Du, B.N., Zannoni, V.G., Laster, L. and Seegmiller,J.E. (1958) The nature of the defect

477   in tyrosine metabolism in alcaptonuria. *J. Biol. Chem.*, **230**, 250–261.

478   2. Garrod, A.E. (1902) The incidence of alkaptonuria: a study in chemical individuality.

479   *Lancet*, **160**, 1616–1620.

480   3. O'Brien, W.M., La Du, B.N. and Bunim, J.J. (1963) Biochemical, pathologic and clinical

481   aspects of alcaptonuria, ochronosis and ochronotic arthropathy. *Am. J. Med.*, **34**, 813–

482   838.

483   4. Phornphutkul, C., Introne, W.J., Perry, M.B., Bernardini, I., Murphey, M.D., Fitzpatrick,

484   D.L., Anderson, P.D., Huizing, M., Anikster, Y., Gerber, L.H., *et al.* (2002) Natural

485   history of alkaptonuria. *N. Engl. J. Med.*, **347**, 2111–2121.

486   5. Helliwell, T.R., Gallagher, J.A. and Ranganath, L. (2008) Alkaptonuria - a review of

487   surgical and autopsy pathology. *Histopathology*, **53**, 503–512.

488   6. Hannoush, H., Introne, W.J., Chen, M.Y., Lee, S.J., O'Brien, K., Suwannarat, P., Kayser,

489   M.A., Gahl, W.A. and Sachdev, V. (2012) Aortic stenosis and vascular calcifications in

490   alkaptonuria. *Mol. Genet. Metab.*, **105**, 198–202.

491   7. Montagutelli, X., Lalouette, A., Coudé, M., Kamoun, P., Forest, M. and Guénet, J.L.

492   (1994) AKU, a mutation of the mouse homologous to human alkaptonuria, maps to

493   chromosome 16. *Genomics*, **19**, 9–11.

494   8. Manning, K., Fernandez-Canon, J.M., Montagutelli, X. and Grompe, M. (1999)

495   Identification of the mutation in the alkaptonuria mouse model. *Hum. Mutat.*, **13**, 171–

496   171.

497   9. Ascher, D.B., Spiga, O., Sekelska, M., Pires, D.E. V., Bernini, A., Tiezzi, M., Kralovicova,

498   J., Borovska, I., Soltysova, A., Olsson, B., *et al.* (2019) Homogentisate 1,2-dioxygenase

499   (HGD) gene variants, their analysis and genotype–phenotype correlations in the largest

500   cohort of patients with AKU. *Eur. J. Hum. Genet.*, **27**, 888–902.

501   10. Zatkova, A., Sedlackova, T., Radvansky, J., Polakova, H., Nemethova, M., Aquaron, R.,

502   Dursun, I., Usher, J.L. and Kadasi, L. (2012) Identification of 11 novel homogentisate

503   1,2 dioxygenase variants in alkaptonuria patients and establishment of a novel LOVD-

504   based HGD mutation database. *JIMD Rep.*, **4**, 55–65.

505   11. Zatkova, A. (2011) An update on molecular genetics of Alkaptonuria (AKU). *J. Inherit.*

506   *Metab. Dis.*, **34**, 1127–1136.

507   12. Fernández-Cañón, J., Granadino, B., Beltrán-Valero de Bernabé, D., Renedo, M.,

508   Fernández-Ruiz, E., Peñalva, M. and Rodríguez de Córdoba, S. (1996) The molecular

509   basis of alkaptonuria. *Nat. Genet.*, **14**, 19–24.

510   13. Laschi, M., Tinti, L., Braconi, D., Millucci, L., Ghezzi, L., Amato, L., Selvi, E.,

511   Spreafico, A., Bernardini, G. and Santucci, A. (2012) Homogentisate 1,2 dioxygenase is

512   expressed in human osteoarticular cells: implications in alkaptonuria. *J. Cell. Physiol.*,

513   **227**, 3254–3257.

514   14. Bernardini, G., Laschi, M., Geminiani, M., Braconi, D., Vannuccini, E., Lupetti, P.,

515   Manetti, F., Millucci, L. and Santucci, A. (2015) Homogentisate 1,2 dioxygenase is

516   expressed in brain: implications in alkaptonuria. *J. Inherit. Metab. Dis.*, **38**, 807–814.

517   15. Ranganath, L.R., Jarvis, J.C., Gallagher, J.A. and Ranganath, L.R. (2013) Recent

518   advances in management of alkaptonuria (invited review; best practice article). *J Clin*

519   *Pathol*, **66**, 367–373.

520   16. Ranganath, L.R., Milan, A.M., Hughes, A.T., Dutton, J.J., Fitzgerald, R., Briggs, M.C.,

521   Bygott, H., Psarelli, E.E., Cox, T.F., Gallagher, J.A., *et al.* (2014) Suitability Of

522   Nitisinone In Alkaptonuria 1 (SONIA 1): an international, multicentre, randomised,

523   open-label, no-treatment controlled, parallel-group, dose-response study to investigate

524   the effect of once daily nitisinone on 24-h urinary homogentisic acid. *Ann. Rheum. Dis.*,

525   **1**, 1–6.

526   17. Ashorn, M., Pitkanen, S., Salo, M.K. and Heikinheimo, M. (2006) Current strategies for

527   the treatment of hereditary tyrosinemia type I. *Pediatr. Drugs*, **8**, 47–54.

528   18. Ranganath, L.R., Khedr, M., Milan, A.M., Davison, A.S., Hughes, A.T., Usher, J.L.,

529   Taylor, S., Loftus, N., Daroszewska, A., West, E., *et al.* (2018) Nitisinone arrests

530   ochronosis and decreases rate of progression of alkaptonuria: evaluation of the effect of

531   nitisinone in the United Kingdom National Alkaptonuria Centre. *Mol. Genet. Metab.*,

532   **125**, 127–134.

533   19. Harding, C.O. (2017) Gene and cell therapy for inborn errors of metabolism. In *Inherited*

534   *Metabolic Diseases*. Springer Berlin Heidelberg, Berlin, Heidelberg, pp. 155–171.

535   20. Brunetti-Pierri, N. (2008) Gene therapy for inborn errors of liver metabolism: progress

536   towards clinical applications. *Ital. J. Pediatr.*, **34**, 2.

537   21. Skarnes, W.C., Rosen, B., West, A.P., Koutsourakis, M., Bushell, W., Iyer, V., Mujica,

538   A.O., Thomas, M., Harrow, J., Cox, T., *et al.* (2011) A conditional knockout resource

539   for the genome-wide study of mouse gene function. *Nature*, **474**, 337–342.

540   22. Collins, F.S. and Rossant, J. (2007) A mouse for all reasons. *Cell*, **128**, 9–13.

541   23. Kühn, R., Schwenk, F., Aguet, M. and Rajewsky, K. (1995) Inducible gene targeting in

542   mice. *Science*, **269**, 1427–1429.

543   24. Milan, A.M., Hughes, A.T., Davison, A.S., Devine, J., Usher, J., Curtis, S., Khedr, M.,

544   Gallagher, J.A. and Ranganath, L.R. (2017) The effect of nitisinone on homogentisic

545   acid and tyrosine: a two-year survey of patients attending the National Alkaptonuria

546   Centre, Liverpool. *Ann. Clin. Biochem.*, **54**, 323–330.

547   25. Yin, H., Xue, W., Chen, S., Bogorad, R.L., Benedetti, E., Grompe, M., Koteliansky, V.,

548   Sharp, P.A., Jacks, T. and Anderson, D.G. (2014) Genome editing with Cas9 in adult

549   mice corrects a disease mutation and phenotype. *Nat. Biotechnol.*, **32**, 551–553.

550   26. Taylor, A.M., Wlodarski, B., Prior, I.A., Wilson, P.J.M., Jarvis, J.C., Ranganath, L.R. and

551   Gallagher, J.A. (2010) Ultrastructural examination of tissue in a patient with

552   alkaptonuric arthropathy reveals a distinct pattern of binding of ochronotic pigment.

553   *Rheumatology*, **49**, 1412–1414.

554   27. Taylor, A.M., Boyde, A., Wilson, P.J., Jarvis, J.C., Davidson, J.S., Hunt, J.A., Ranganath,

555   L.R. and Gallagher, J.A. (2011) The role of calcified cartilage and subchondral bone in

556   the initiation and progression of ochronotic arthropaththy in alkaptonuria. *Arthritis*

557   *Rheum.*, **63**, 3887–3896.

558   28. Tinti, L., Taylor, A.M., Santucci, A., Wlodarski, B., Wilson, P.J., Jarvis, J.C., Fraser,

559   W.D., Davidson, J.S., Ranganath, L.R. and Gallagher, J.A. (2011) Development of an in

560   vitro model to investigate joint ochronosis in alkaptonuria. *Rheumatology*, **50**, 271–277.

561   29. Millucci, L., Braconi, D., Bernardini, G., Lupetti, P., Rovensky, J., Ranganath, L. and

562   Santucci, A. (2015) Amyloidosis in alkaptonuria. *J. Inherit. Metab. Dis.*, **38**, 797–805.

563   30. Preston, A.J., Keenan, C.M., Sutherland, H., Wilson, P.J., Wlodarski, B., Taylor, A.M.,

564   Williams, D.P., Ranganath, L.R., Gallagher, J.A. and Jarvis, J.C. (2014) Ochronotic

565   osteoarthropathy in a mouse model of alkaptonuria, and its inhibition by nitisinone. *Ann.*

566   *Rheum. Dis.*, **73**, 284–289.

567   31. Justice, M.J., Noveroske, J.K., Weber, J.S., Zheng, B. and Bradley, A. (1999) Mouse

568   ENU mutagenesis. *Hum. Mol. Genet.*, **8**, 1955–1963.

569   32. Crawford, L.W., Foley, J.F. and Elmore, S.A. (2010) Histology atlas of the developing

570   mouse hepatobiliary system with emphasis on embryonic days 9.5-18.5. *Toxicol.*

571   *Pathol.*, **38**, 872–906.

572   33. Sasaki, K. and Sonoda, Y. (2000) Histometrical and three-dimensional analyses of liver

573   hematopoiesis in the mouse embryo. *Arch. Histol. Cytol.*, **63**, 137–146.

574   34. Takemura, T., Yoshida, Y., Kiso, S., Saji, Y., Ezaki, H., Hamano, M., Kizu, T., Egawa,

575   M., Chatani, N., Furuta, K., *et al.* (2013) Conditional knockout of heparin-binding

576   epidermal growth factor-like growth factor in the liver accelerates carbon tetrachloride-

577   induced liver injury in mice. *Hepatol. Res.*, **43**, 384–393.

578   35. Kobak, A.C., Oder, G., Kobak, Ş., Argin, M. and Inal, V. (2005) Ochronotic arthropathy:

579   disappearance of alkaptonuria after liver transplantation for hepatitis B-related cirrhosis.

580   *J. Clin. Rheumatol.*, **11**, 323–325.

581   36. Introne, W.J., Phornphutkul, C., Bernardini, I., McLaughlin, K., Fitzpatrick, D. and Gahl,

582   W.A. (2002) Exacerbation of the ochronosis of alkaptonuria due to renal insufficiency

583   and improvement after renal transplantation. *Mol. Genet. Metab.*, **77**, 136–142.

584   37. Krechowec, S.O., Burton, K.L., Newlaczyl, A.U., Nunn, N., Vlatković, N. and Plagge, A.

585   (2012) Postnatal changes in the expression pattern of the imprinted signalling protein

586   XLαs underlie the changing phenotype of deficient mice. *PLoS One*, **7**, e29753.

587   38. Hughes, A.T., Milan, A.M., Christensen, P., Ross, G., Davison, A.S., Gallagher, J.A.,

588   Dutton, J.J. and Ranganath, L.R. (2014) Urine homogentisic acid and tyrosine:

589   simultaneous analysis by liquid chromatography tandem mass spectrometry. *J.*

590   *Chromatogr. B*, **963**, 106–112.

591   39. Hughes, A.T., Milan, A.M., Davison, A.S., Christensen, P., Ross, G., Gallagher, J.A.,

592   Dutton, J.J. and Ranganath, L.R. (2015) Serum markers in alkaptonuria: simultaneous

593   analysis of homogentisic acid, tyrosine and nitisinone by liquid chromatography tandem

594   mass spectrometry. *Ann. Clin. Biochem.*, **52**, 597–605.

595   40. Frost, S.L., Liu, K., Li, I.M.H., Poulet, B., Comerford, E., De Val, S. and Bou-Gharios,

596   G. (2018) Multiple enhancer regions govern the transcription of CCN2 during

597   embryonic development. *J. Cell Commun. Signal.*, **12**, 231–243.

598   41. Taylor, A.M., Preston, A.J., Paulk, N.K., Sutherland, H., Keenan, C.M., Wilson, P.J.M.,

599   Wlodarski, B., Grompe, M., Ranganath, L.R., Gallagher,J.A., *et al.* (2012) Ochronosis in

600   a murine model of alkaptonuria is synonymous to that in the human condition.

601   *Osteoarthr. Cartil.*, **20**, 880–886.

602   42. Kranz, A., Fu, J., Duerschke, K., Weidlich, S., Naumann, R., Stewart, A.F. and

603   Anastassiadis, K. (2010) An improved Flp deleter mouse in C57Bl/6 based on Flpo

604   recombinase. *Genesis*, **48**, 512–520.

605   43. Moriya, K., Bae, E., Honda, K., Sakai, K., Sakaguchi, T., Tsujimoto, I., Kamisoyama, H.,

606   Keene, D.R., Sasaki, T. and Sakai, T. (2011) A fibronectin-independent mechanism of

607   collagen fibrillogenesis in adult liver remodeling. *Gastroenterology*, **140**, 1653–1663.

608   44. Norman, B.P., Davison, A.S., Ross, G.A., Milan, A.M., Hughes, A.T., Sutherland, H.,

609   Jarvis, J.C., Roberts, N.B., Gallagher, J.A. and Ranganath, L.R. (2019) A

610   comprehensive LC-QTOF-MS metabolic phenotyping strategy: application to

611   alkaptonuria. *Clin. Chem.*, **65**, 530–539.

612

613

614

615

616

617

618

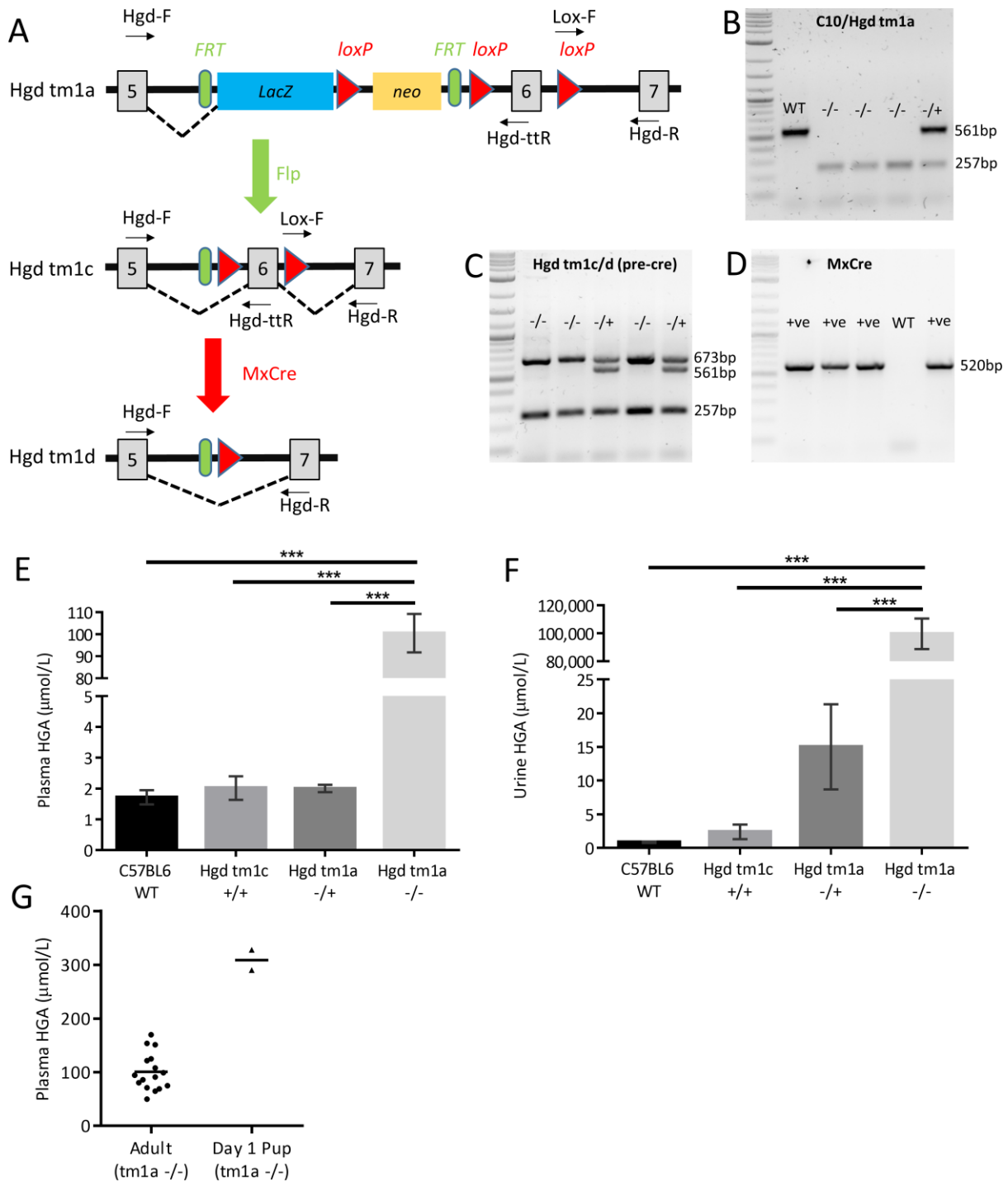619

620

621

622

623

624

625

626

627

628

629

630   <u>Figures and Legends</u>

632   Figure 1. Phenotyping of Hgd tm1a mice. A-D shows genotyping of the modified HGD

633   allele. A schematic of the modified HGD allele is shown in A. Hgd tm1a: AKU phenotype.

634   Hgd tm1c: wildtype phenotype. Hgd tm1d: liver-specific and inducible KO. Using primer

635   pairs Hgd-F/Hgd-ttR and Lox-F/Hgd-R, B shows the genotyping of tm1a; C shows the

27

636   genotyping of tm1c (after flp recombination) and tm1d (before cre recombination). D shows

637   the genotyping of MxCre. A 2-log DNA ladder was used in B-D. E-H show elevation of

638   HGA in Hgd tm1a -/-. E and F show plasma and urine HGA. Plasma HGA is elevated

639   approximately 100-fold in Hgd tm1a -/- mice (n=16) compared to C57BL/6 wildtype (n=4),

640   Hgd tm1c +/+ (n=7) and Hgd tm1a -/+ (n=18) controls. Urinary HGA is elevated

641   approximately 10,000-100,000-fold in Hgd tm1a -/- mice (n=19) compared with C57BL/6

642   wildtype (n=7), Hgd tm1c +/+ (n=7) and Hgd tm1a -/+ (n=19) controls. G shows HGA levels

643   in day 1 Hgd tm1a -/- pups (2 pools of n=3) compared with adults (n=16). HGA =

644   homogentisic acid. Significance: $p<0.05$ *, $p<0.01$ ** and $p<0.001$ ***. Error bars represent

645   SEM.
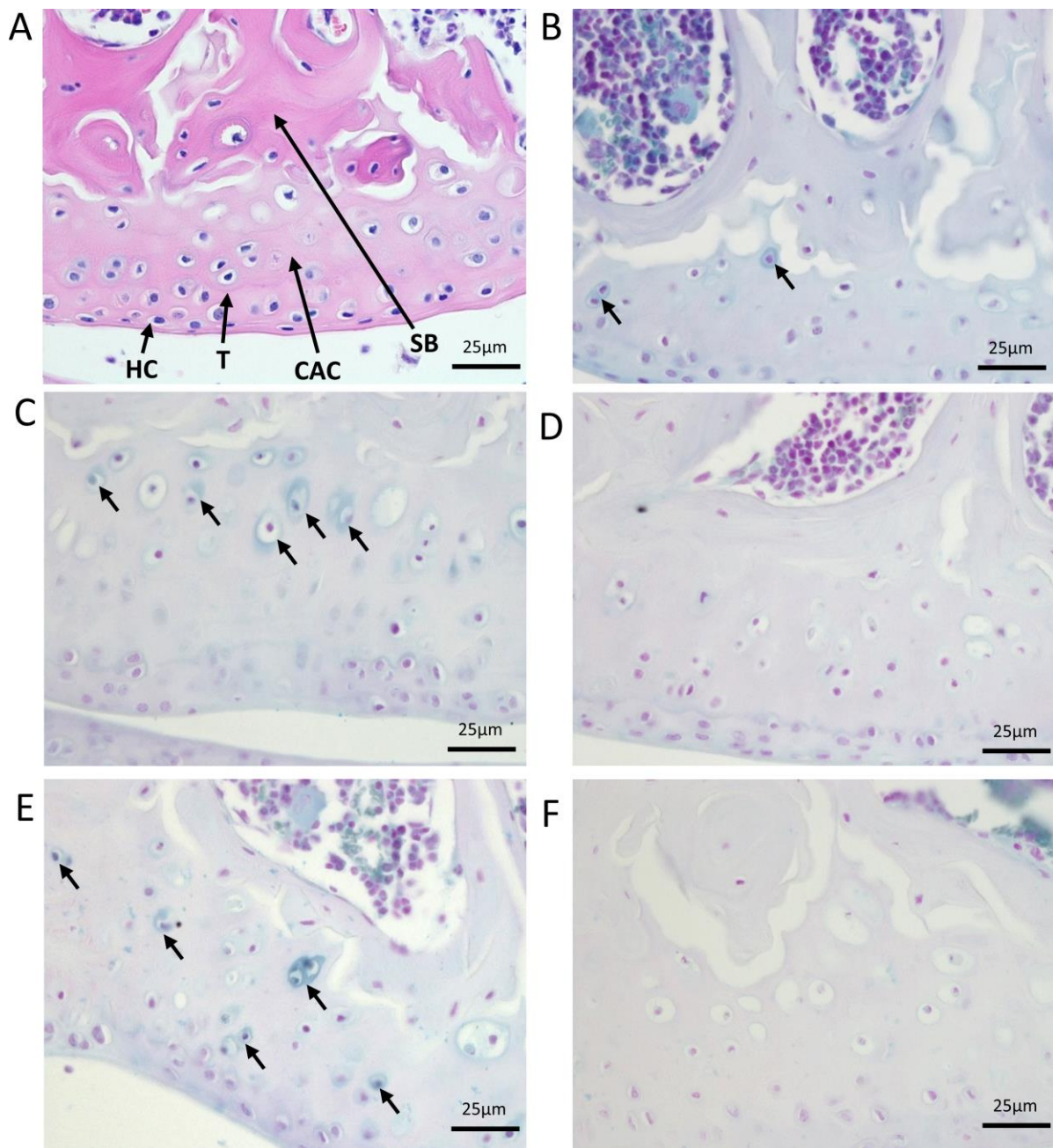
Figure 2. Initiation and progression of ochronosis in Hgd tm1a mice. H+E staining in A shows division of articular cartilage into different zones: hyaline cartilage (HC) and calcified articular cartilage (CAC) separated by the tidemark (T). Deep to calcified articular cartilage is subchondral bone (SB). B–F show femoral condyles from Hgd tm1a mice that have been Schmorl's stained (stains ochronotic pigment a blue colour). B shows pericellular pigmentation of chondrons situated in the calcified articular cartilage in a 9 week Hgd tm1a -/- femoral condyle. C and E show the femoral condyle of Hgd tm1a -/- mice at 26 and 40

654   weeks respectively. The pigmentation has advanced to the inner compartment of the cell,

655   with more numerous affected chondrocytes showing varying pigment intensities. The

656   pigmentation is still confined to the calcified articular cartilage layer. Hgd tm1a -/+ mice at

657   26 and 40 weeks (D and F respectively) show no pigmentation. All sections: 6μM.

658

659

660
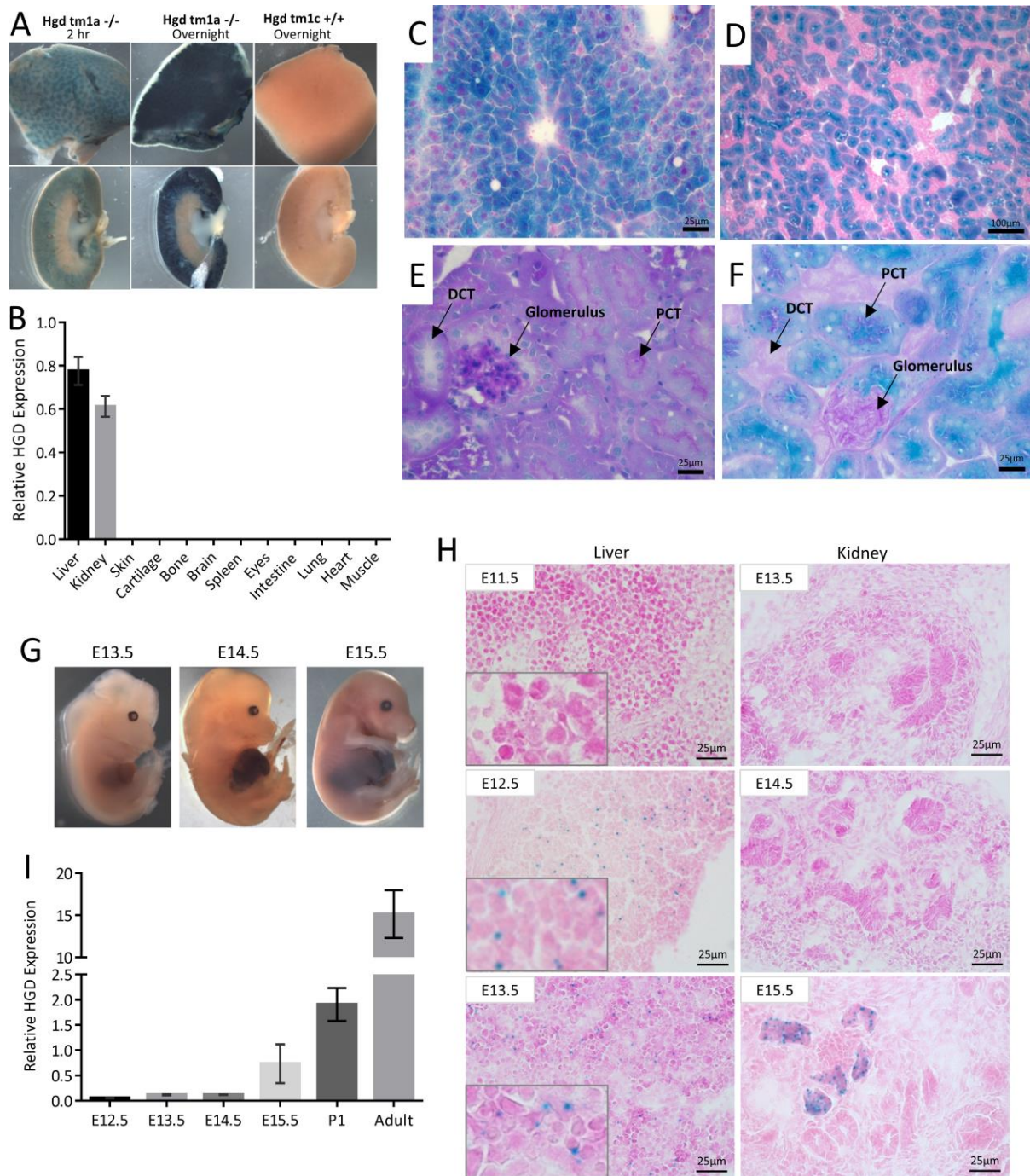
Figure 3. Localisation of HGD expression. A shows LacZ staining in adult liver (top row) and kidney (bottom row). LacZ blue staining blue represents HGD expression seen only in the liver parenchyma and kidney cortex of Hgd tm1a -/- adult mice. Control Hgd tm1c +/+ liver and kidney were LacZ negative. B shows HGD mRNA across a variety of adult Hgd tm1d WT tissues analysed via qPCR (HGD1 primers). C-F shows frozen section staining of adult liver and kidney from Hgd tm1a -/- mice, with liver (C) and kidney cortex (D) showing

31

667   specific LacZ staining after 2 hours. In E, PAS staining distinguishes PCTs from DCTs by

668   the presence of a PAS-positive dark pink/purple brush border. In F, the LacZ blue cells

669   localise with the PAS-positive PCT cells. G-I shows HGD expression in Hgd tm1a -/-

670   embryos. G shows whole time-mated embryo LacZ staining, with positive staining seen at

671   E14.5 in the liver. H shows microscopic frozen section LacZ staining of liver and kidney.

672   Positive staining is seen at E12.5 onwards in liver and from E15.5 in kidney. I shows HGD

673   mRNA (HGD1 primers) in E12.5 (n=3), E13.5 (n=3), E14.5 (n=4) and E15.5 (n=3) embryos,

674   day 1 pups (P1) (n=6) and adult Hgd tm1a -/- mice (n=4). All sections: 6/7µM. PAS: Periodic

675   acid Schiff. PCT = proximal convoluted tubule. DCT: distal convoluted tubule. Error bars

676   represent SEM. HGD expression normalised to 18S.

677

678
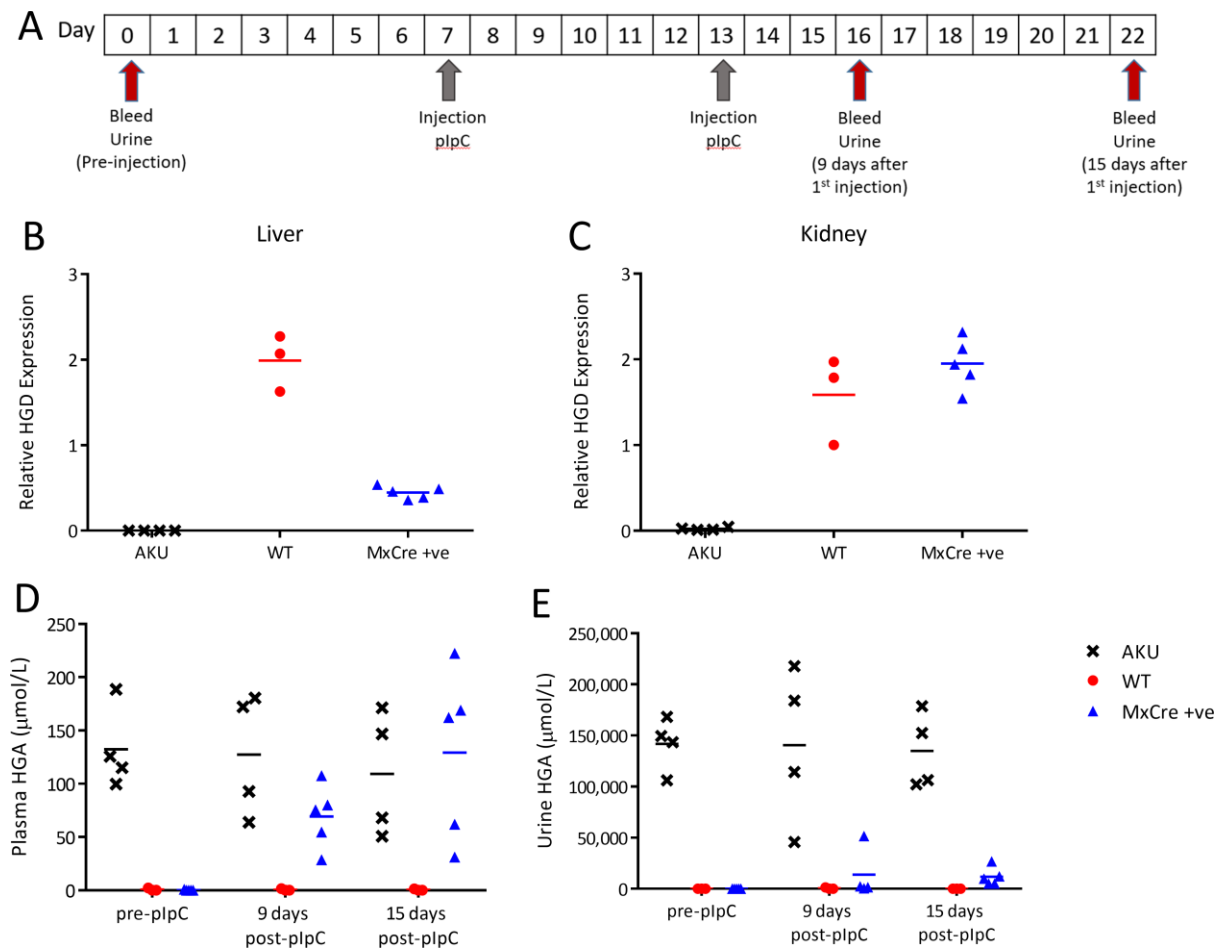
679

680   Figure 4. Liver-specific HGD knockout, induced by pIpC injection, in Hgd tm1d MxCre +ve

681   mice. A, shows the timescale of blood and urine sampling and pIpC injections. B and C show

682   HGD mRNA (HGD2 primers; relative to 18S) in Hgd tm1a -/- (AKU controls, n=4), Hgd

683   tm1d MxCre WT (wildtype controls, n=3) and Hgd tm1d MxCre +ve mice (MxCre +ve, n=5)

684   in the liver and kidney respectively, 15 days after pIpC injection. MxCre +ve mice show

685   reduced liver, but not kidney, HGD expression compared to wildtype controls. D and E show

686   plasma and urine HGA, respectively, pre-injection, 9 and 15 days after pIpC injection. Pre-

687   injection, HGA in the plasma is not detected in MxCre +ve or WT mice. Hgd tm1a -/- mice

688   show high HGA. Post-pIpC, plasma HGA in MxCre +ve mice is increased. Pre-injection,

689   urinary HGA is low in MxCre +ve and WT mice compared to Hgd tm1a -/-. Post-pIpC,

690   urinary HGA shows a relatively small increase in MxCre +ve mice.

691
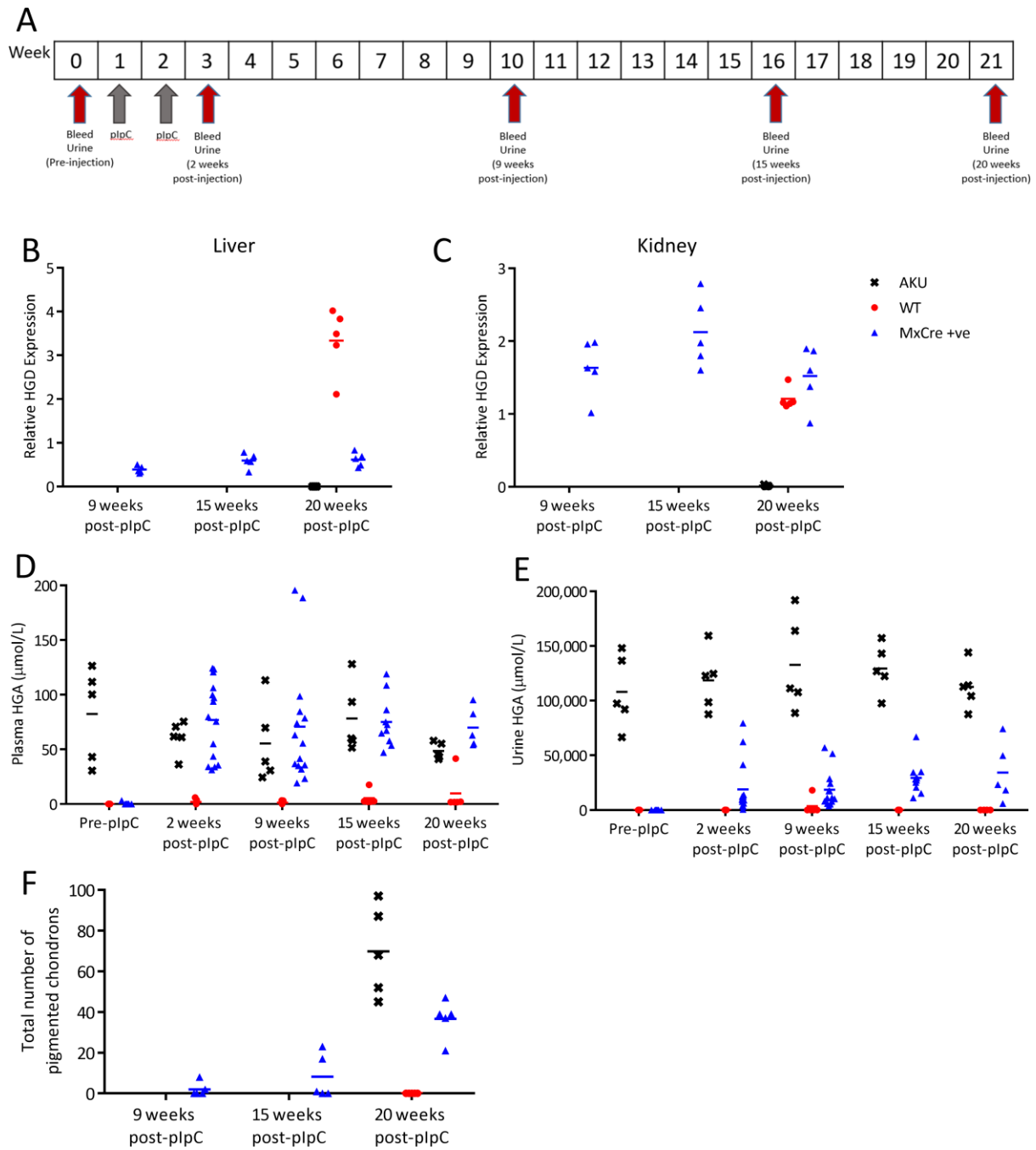
Figure 5. Long-term follow up of Hgd tm1d MxCre +ve mice injected with pIpC. A shows

the timescale of blood and urine sampling and pIpC injections. Hgd tm1a -/- were injected

with pIpC (AKU controls, n=5). Hgd tm1d MxCre +ve were injected with PBS (wildtype

controls, n=5). Hgd tm1d MxCre +ve mice were injected with pIpC (MxCre +ve, n=15). B

and C show relative HGD mRNA (HGD2 primers; relative to 18S) in the liver and kidney

respectively, of MxCre +ve mice at 9, 15 and 20 weeks after the first injection, and in AKU

698   and wildtype controls at 20 weeks. Liver HGD mRNA was reduced, compared to wildtype

699   controls, in MxCre +ve mice at 9 weeks and was sustained until 20 weeks. Kidney expression

700   was not reduced by pIpC injection in MxCre +ve mice. D and E show plasma and urine HGA

701   levels respectively, pre-injection, and at 2, 9, 15 and 20 weeks post-injection. Pre-injection,

702   plasma HGA is not detected in MxCre +ve or WT mice and AKU mice showed elevated

703   HGA. Post-pIpC, plasma HGA in MxCre +ve mice was increased at 2 weeks and remained at

704   this level until 20 weeks. Pre-injection, urinary HGA is low in MxCre +ve and WT mice

705   compared with AKU controls. Post-pIpC, urinary HGA showed a relatively small increase in

706   MxCre +ve mice compared with AKU controls. The total number of pigmented chondrons in

707   a representative section of the knee joint, stained with Schmorl's, is shown in F, at 9, 15 and

708   20 weeks post-injection.

709
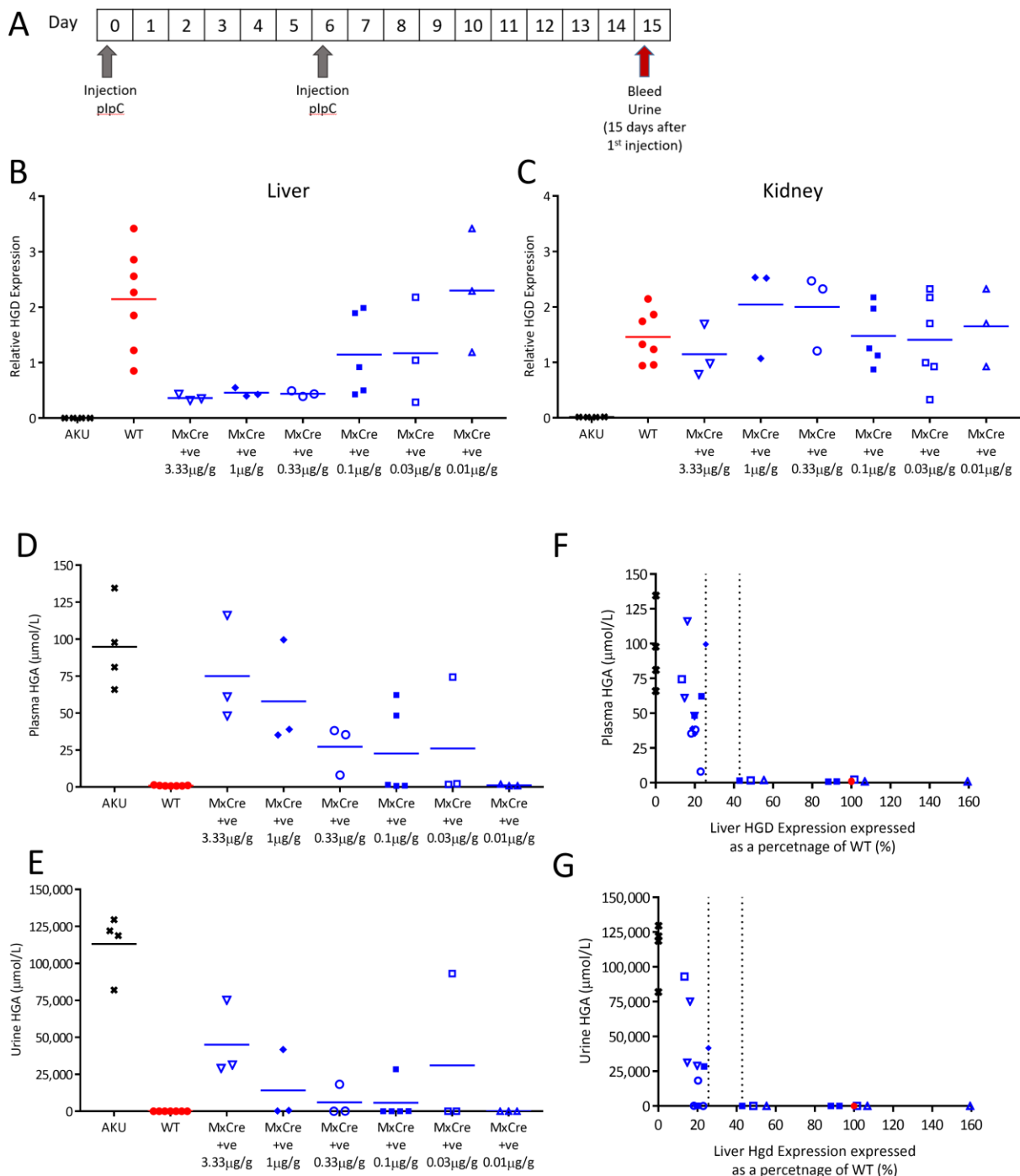
Figure 6. Liver-specific HGD knockout, induced by decreasing doses of pIpC, in Hgd tm1d

MxCre +ve mice. A, shows the timescale of blood and urine sampling and injections of pIpC.

B and C show relative HGD expression (HGD2 primers; relative to 18S) in Hgd tm1a -/-

(AKU controls, n=4), Hgd tm1d MxCre WT (wildtype controls, n=7) and Hgd tm1d MxCre

+ve mice (3.33µg/g, n=3; 0.1µg/g, n=3; 0.33µg/g, n=3; 0.1µg/g, n=5; 0.03µg/g, n=3;

715   0.01µg/g, n=3) in the liver and kidney respectively, 15 days post-pIpC. Varying the dose of

716   pIpC resulted in a range of liver HGD expression in the MxCre +ve mice, with lower doses

717   resulting in higher HGD expression. Kidney HGD expression was unchanged by pIpC. D and

718   E show plasma and urine HGA, respectively, 15 days post-pIpC. A dose response in HGA

719   was observed in both the plasma and the urine of MxCre +ve mice, with higher pIpC doses

720   resulting in more elevated HGA. HGA was elevated in Hgd tm1a -/- and was low in wildtype

721   controls. F and G show the relationship between liver HGD mRNA (expressed as a

722   percentage of the mean wildtype level) with plasma and urinary HGA respectively, 15 days

723   post-pIpC.

724
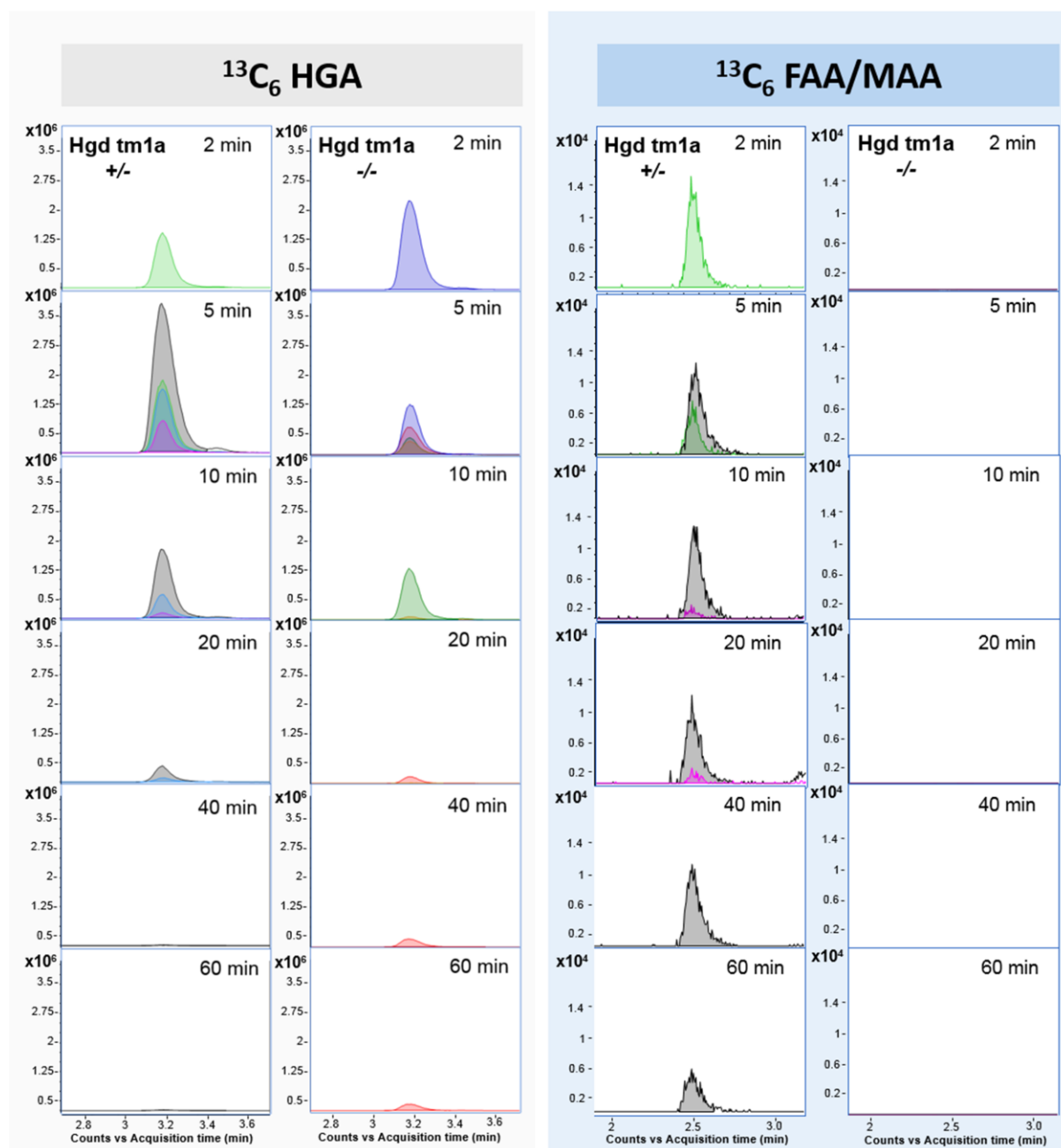
Figure 7. LC-QTOF-MS plasma flux analysis data acquired following injection of Hgd tm1a -/- and Hgd tm1a -/+ mice with $^{13}C_6$-HGA. Plots show extracted ion chromatograms (theoretical accurate mass ±5 ppm) for $^{13}C_6$-HGA and $^{13}C_6$-fumarylacetoacetic acid (FAA)/$^{13}C_6$-maleylacetoacetic acid (MAA). Traces are for individual plasma samples taken 2-60 minutes post-injection and colour-coded to represent individual mice. $^{13}C_6$-HGA was detected in Hgd tm1a -/- and Hgd tm1a -/+ indicating presence of the tracer. $^{13}C_6$-MAA/FAA

731   was observed at 2-60 minutes post-injection in Hgd tm1a -/+, and was not observed in Hgd

732   tm1a -/- at any time point.

733

734   **Abbreviations**: AKU, alkaptonuria; ENU, N-ethyl-N-nitrosourea; FAA, fumarylacetoacetic

735   acid; FAH, fumarylacetoacetate hydroxylase; HT-1, hereditary tyrosinaemia type I; HGA,

736   homogentisic acid; HGD, homogentisate 1,2-dioxygenase; HPLC, high performance liquid

737   chromatography; HPPD, 4-hydroxyphenylpyruvate dioxygenase; MAA, maleylacetoacetic

738   acid; NTBC, 2-(2-nitro-4-trifluoromethylbenzoyl)-1,3-cyclohexanedione; PCT; proximal

739   convoluted tubule; pIpC, polyinosinic:polycytidylic acid.

740